Electronic Supplementary Material (ESI) for Nanoscale.

Rapid improvement of heart repair after myocardial infarction by precise magnetic stimulation on vagus nerve with injectable magnetic hydrogel

Supplementary information

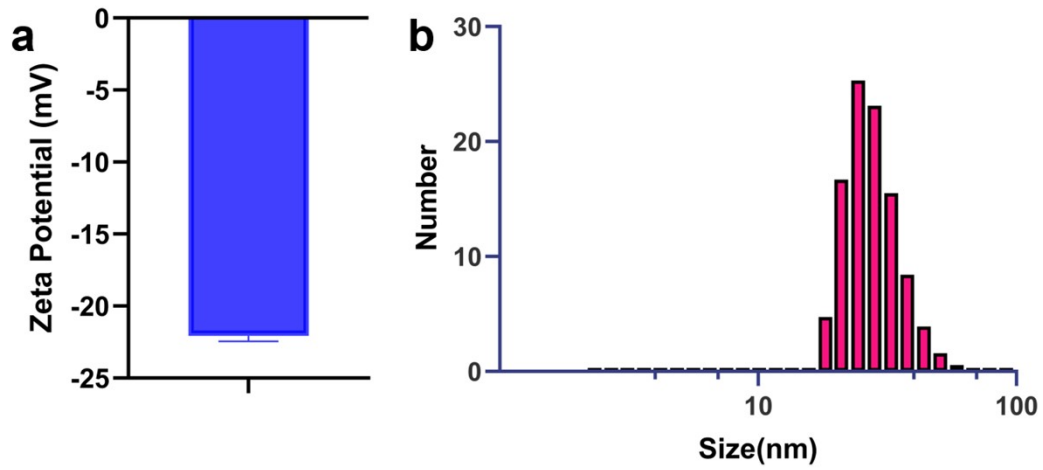

Figure S1 Characterization of SPIO nanoparticles. (a) Zeta potential of SPIO nanoparticles. (b) Particle size distribution of SPIO nanoparticles.

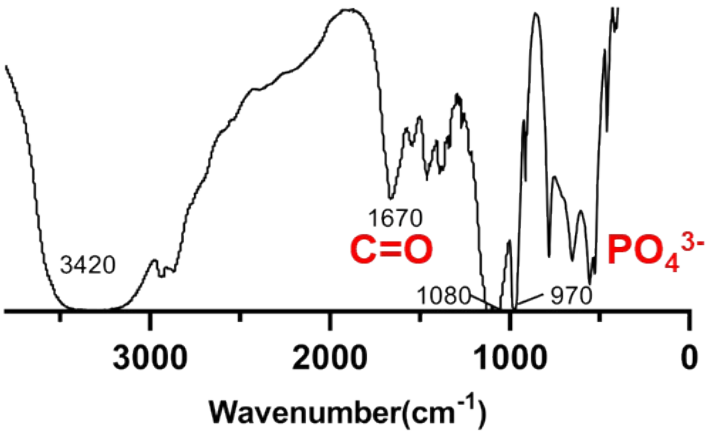

Figure S2 FTIR of SPIO-CS/GP hydrogel.

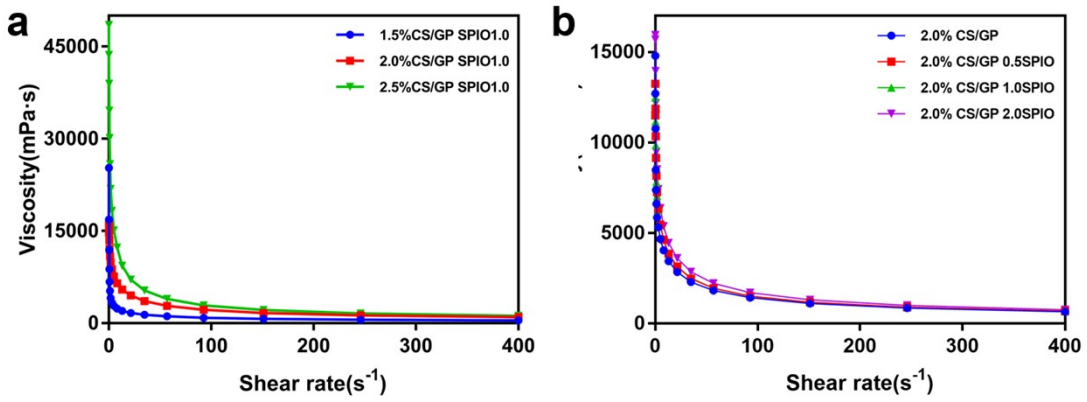

Figure S3 Viscosity of different SPIO-CS/GP hydrogels with shear rate ranging from 0.1-400 s^{-1}. (a) Viscosity of SPIO-CS/GP hydrogels prepared with different chitosan concentrations. (b) Viscosity of SPIO-CS/GP hydrogels prepared with different SPIO nanoparticle concentrations.

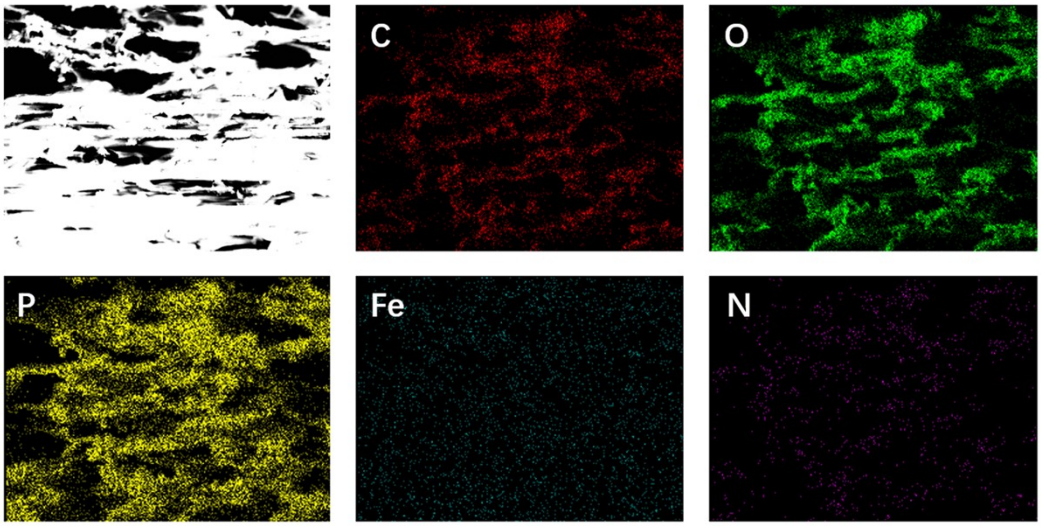

Figure S4 Elemental distribution of SPIO-CS/GP hydrogels, including C, O, P, Fe and N elements.

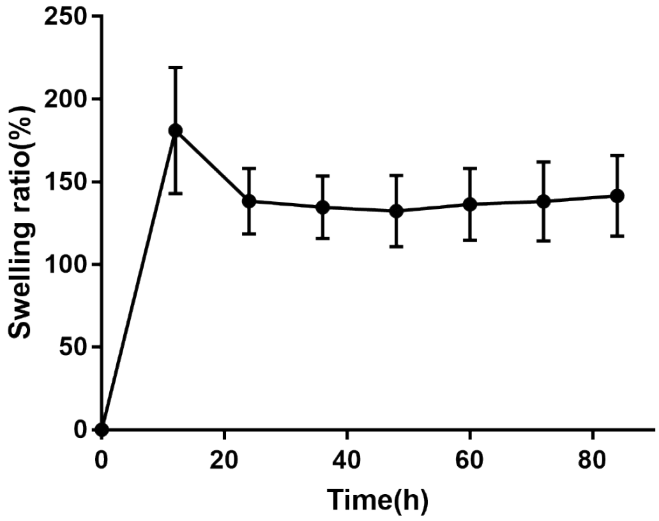

Figure S5 Changes in the swelling rate of SPIO-CS/GP hydrogels over 84 hours.

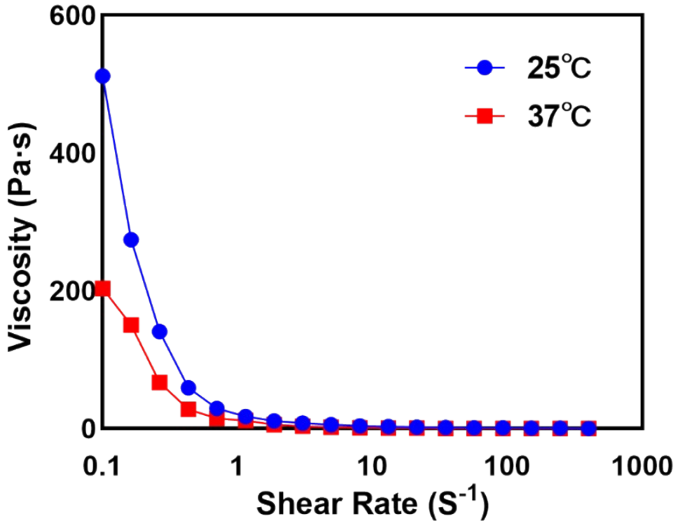

Figure S6 Viscosity change of SPIO-CS/GP hydrogels with shear rate ranging from 0.1-400 s^{-1} at 25°C and 37°C.

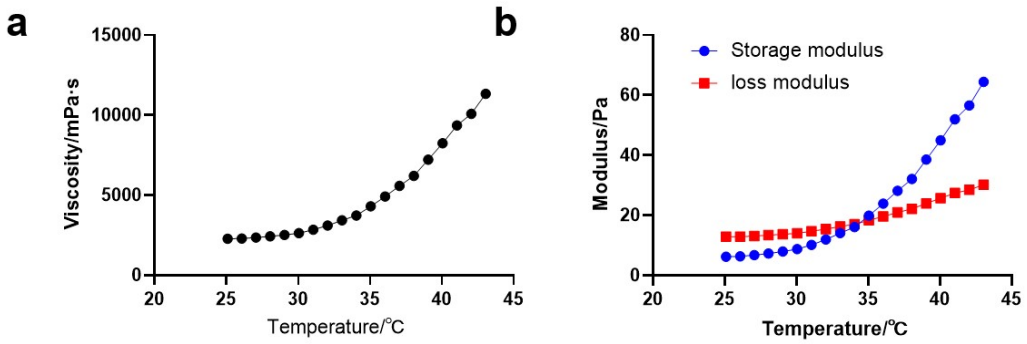

Figure S7 Viscoelastic properties of SPIO-CS/GP hydrogels. (a) Viscosity of SPIO-CS/GP hydrogel as a function of temperature. (b) Modulus of SPIO-CS/GP hydrogel as a function of temperature.

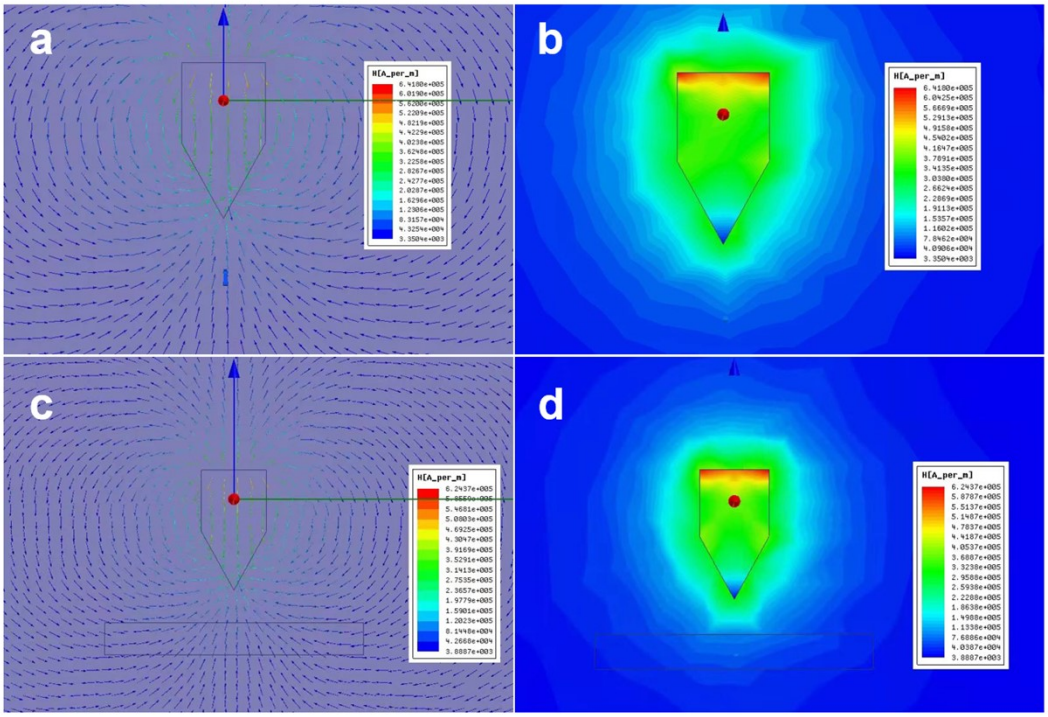

Figure S8 Simulated distribution of magnetic field intensity. (a,b) subuliform magnet alone; (c,d) subuliform magnet combined with a square muscular tissue.

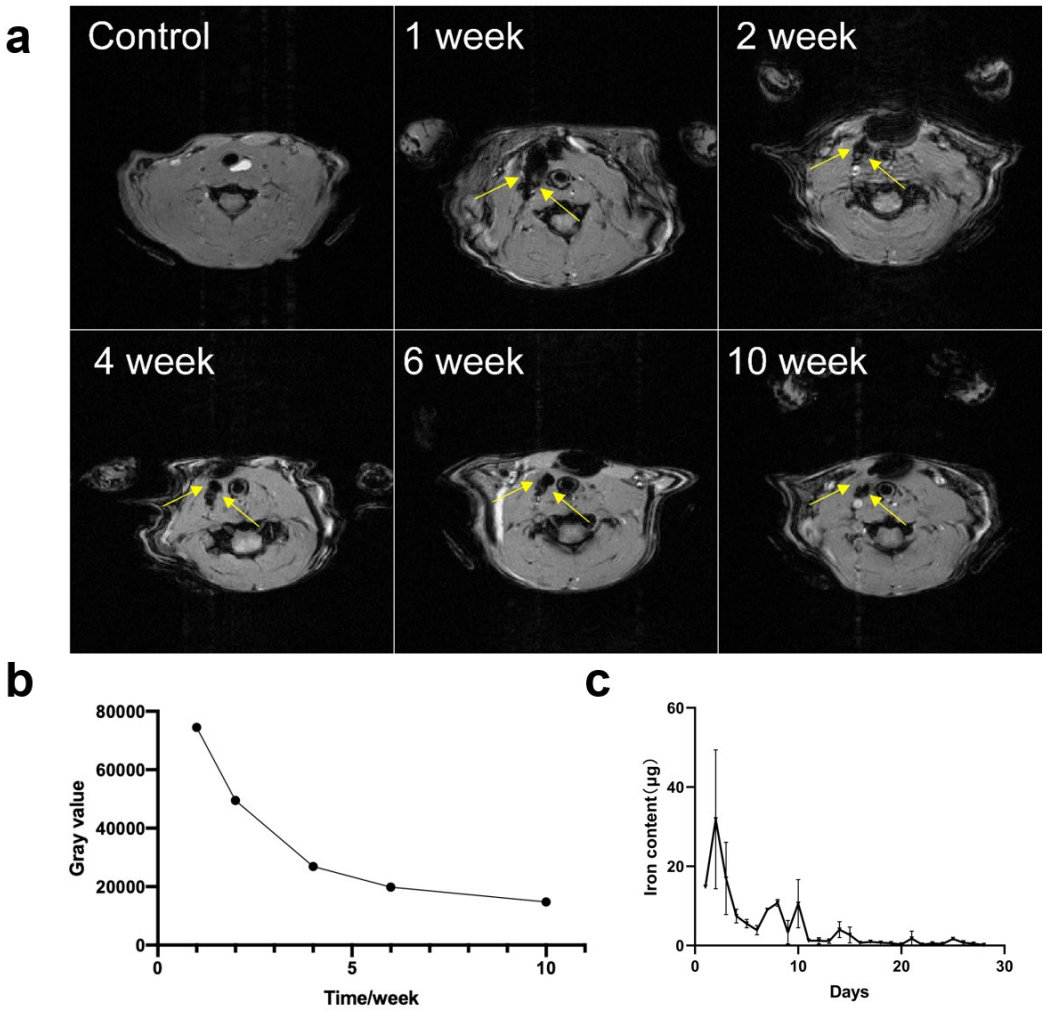

Figure S9 *In vivo* metabolism of SPIO-CS/GP hydrogels. (a) MRI images of SPIO-CS/GP hydrogel in vivo at various moments. (b) grayscale statistics of MRI images. (c) Content of Fe in the feces of rats implanted with the hydrogel.

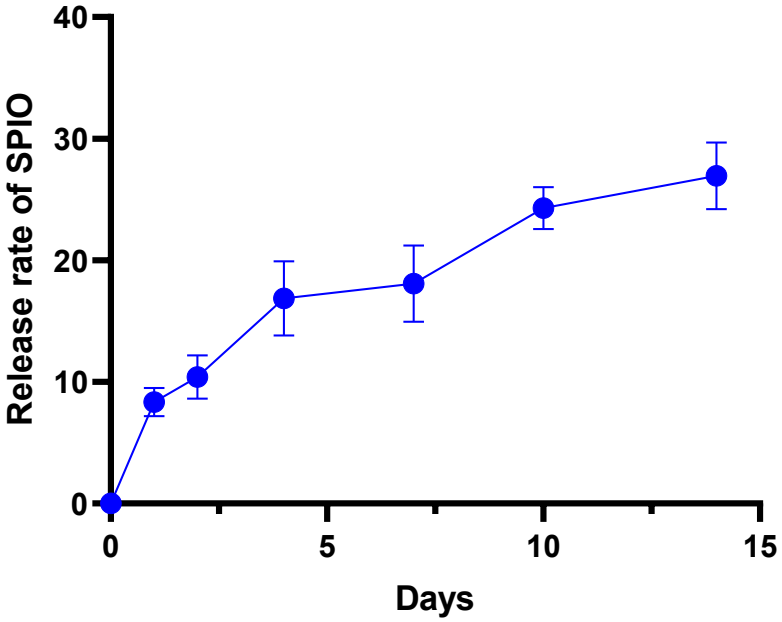

Figure S10 Release rate of SPIO in hydrogel at 37°C for 14 days.

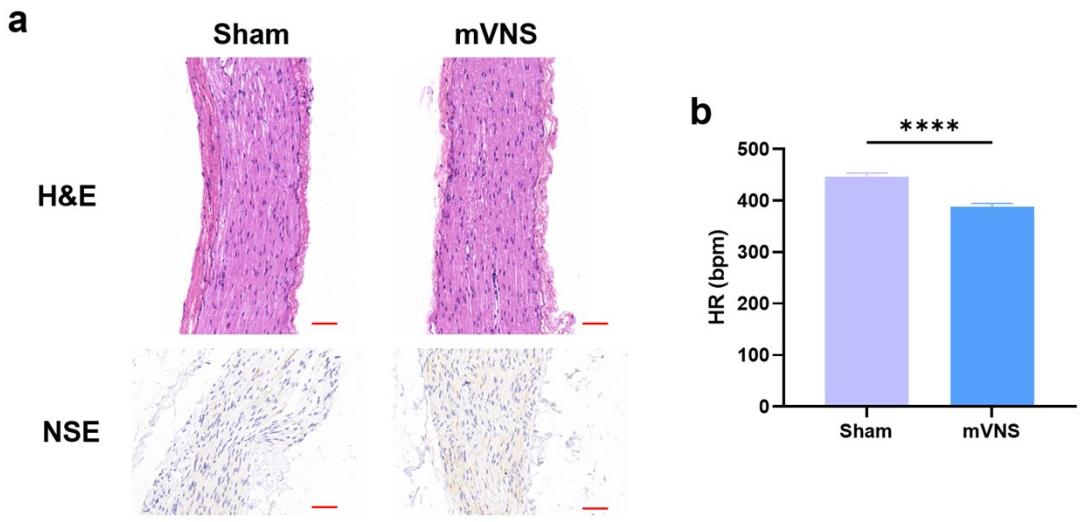

Figure S11 Application of magnetic stimulation for 4 weeks, (a) H&E and NSE (Scale bar = 50 μm) staining of the vagus nerve; (b) heart rate changes in rats. $p < 0.05$ was considered statistically significant. (****indicate $p < 0.0001$).

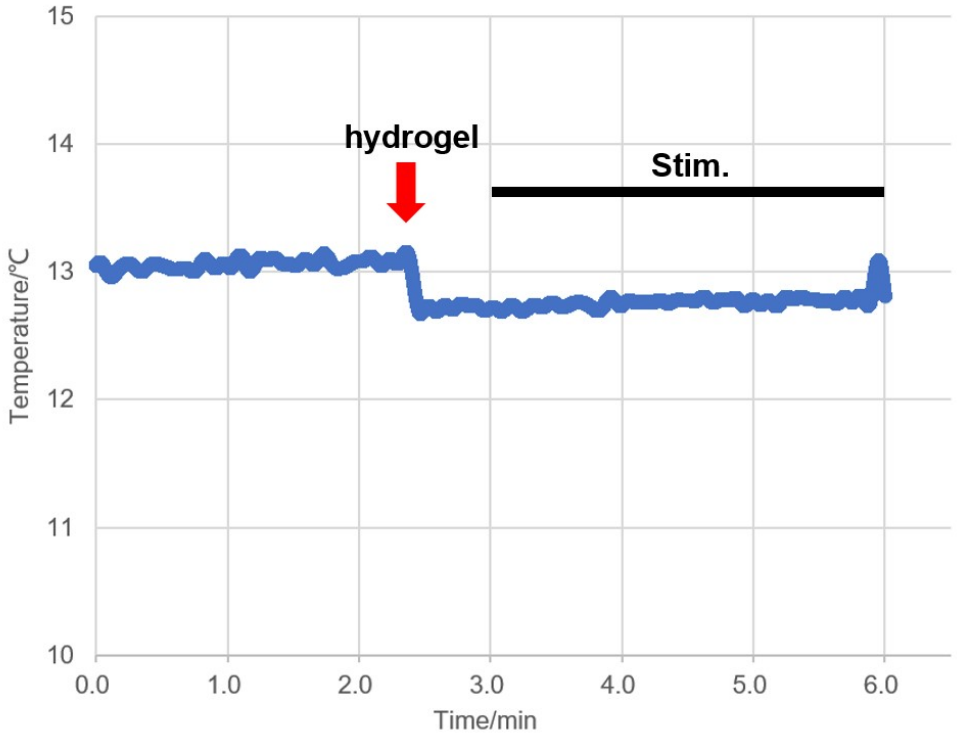

Figure S12 Temperature variation of SPIO-CS/GP hydrogels under the action of a rotating magnetic field.

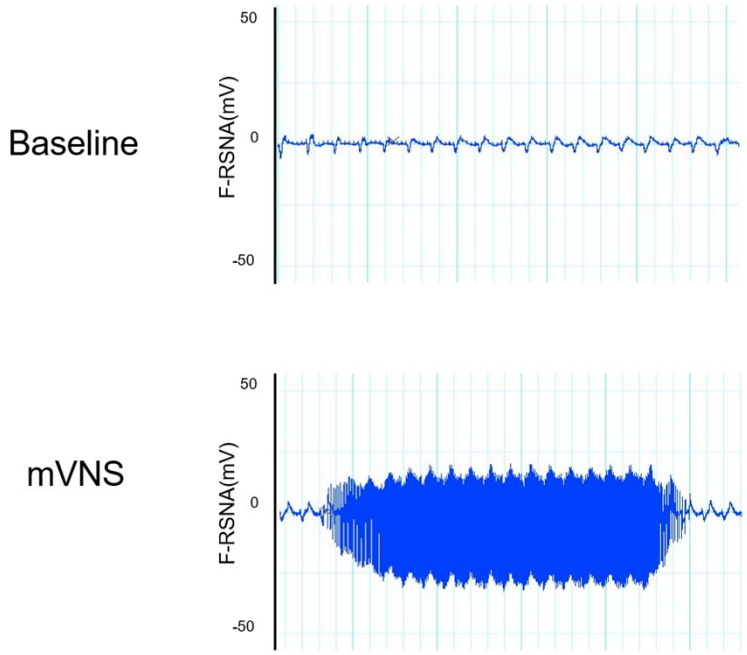

Figure S13 Neural potential recordings in the resting state and after magnetic stimulation.

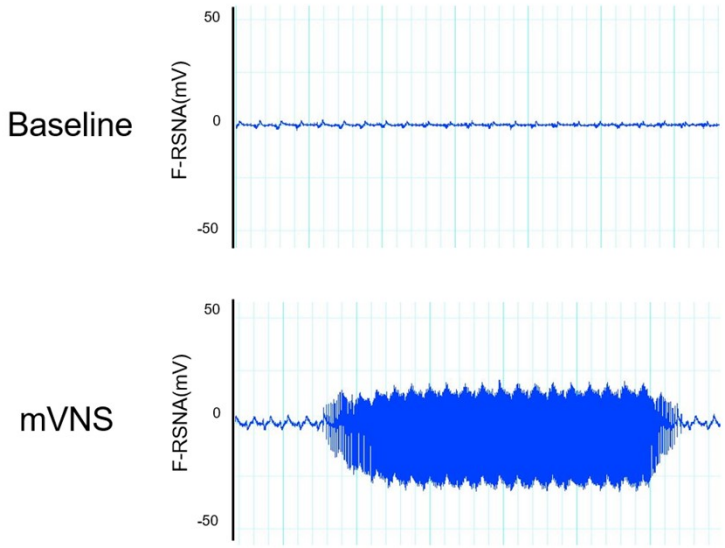

Figure S14 Neural potential changes after activation of the left vagus nerve by the mVNS system.

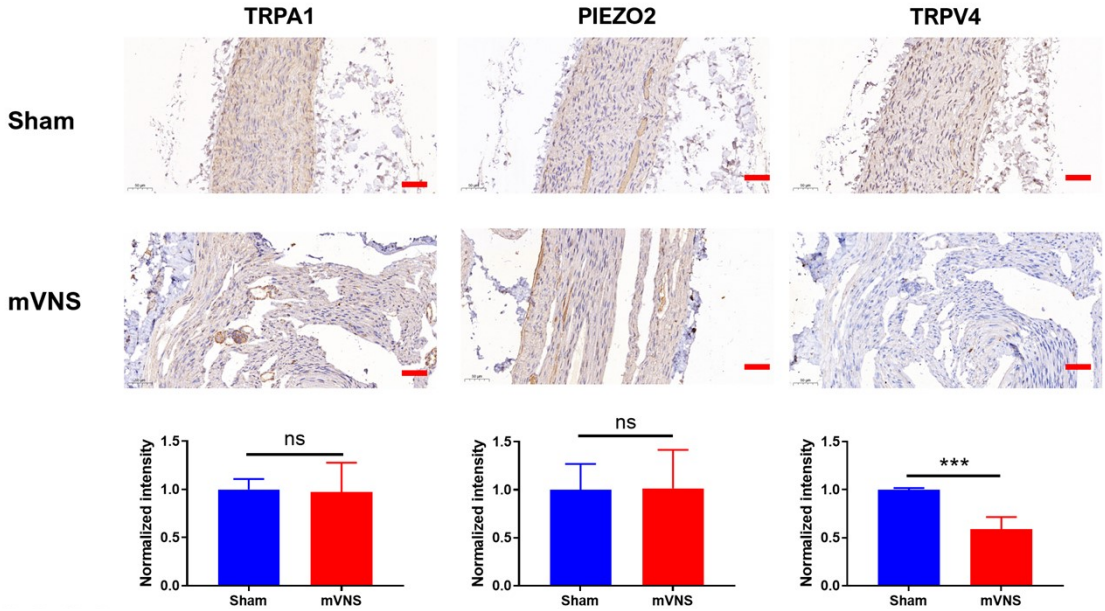

Figure S15 Staining and statistical images of the expression of TRPA1, PIEZO2 and TRPV4 ion channels after magnetic stimulation (Scale bar=50 μm). $p < 0.05$ was considered statistically significant. NS means not significant between groups. (* indicate $p < 0.05$, * * * indicate $p < 0.001$).

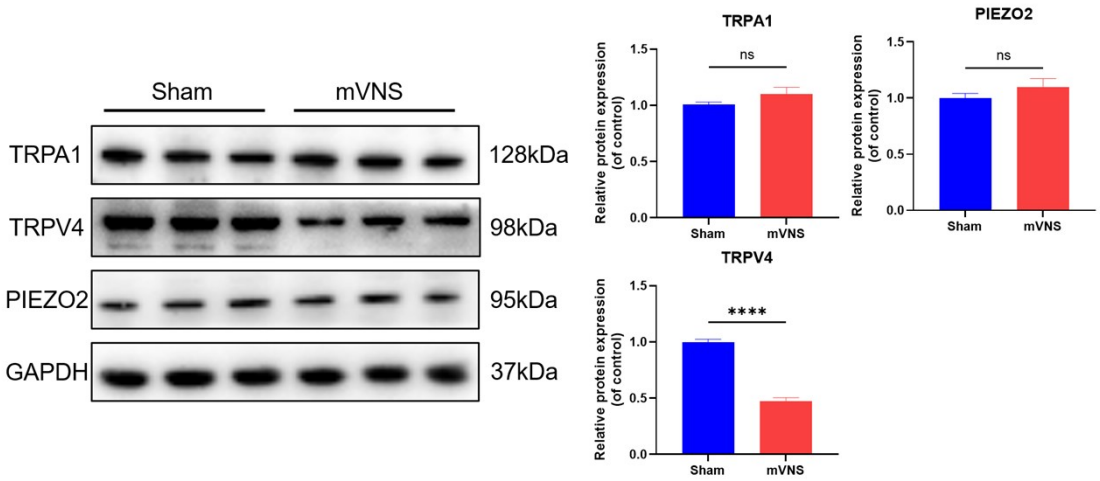

Figure S16 Western blot analysis of protein levels of TRPA1, PIEZO2 and TRPV4 in vagus nerve (left) and quantification (right, n = 6 per group). GAPDH as an internal control. Data are mean ± SEM. ****P < 0.001; All P values were obtained by Student's t-test.

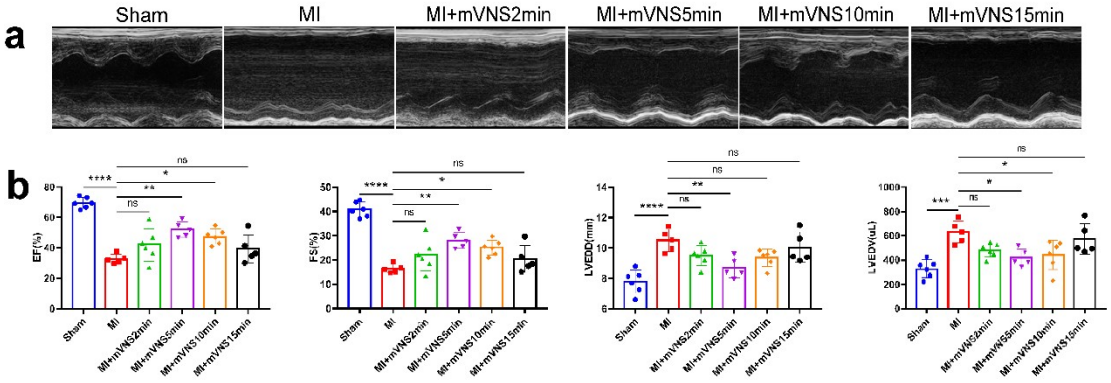

Figure S17 Effects of different vagus nerve magnetic stimulation times on cardiac function in rats with myocardial infarction. (a) Echocardiography and (b) Cardiac function parameters of rats with different vagus nerve magnetic stimulation times. $p < 0.05$ was considered statistically significant. NS means not significant between groups. (* indicate $p < 0.05$, * * indicate $p < 0.01$, * * * indicate $p < 0.001$, and **** indicate $p < 0.0001$).

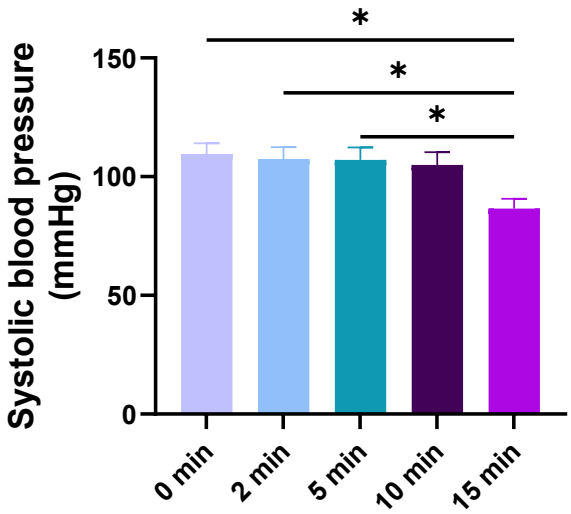

Figure S18 Effect of different magnetic stimulation times on systolic blood pressure.